A Review on Mechanical Properties and Response of Fibre Metal Laminate under Impact Loading (Experiment)

Murni Awi[1], Ahmad Sufian Abdullah[2,*]

[1]Centre for Mechanical Engineering Studies, Universiti Teknologi MARA, Cawangan Pulau Pinang, Permatang Pauh, Pulau Pinang, 13500, Malaysia

[2]Advanced Mechanics Research Group, Centre for Mechanical Engineering Studies, Universiti Teknologi MARA, Cawangan Pulau Pinang, Permatang Pauh, Pulau Pinang, 13500, Malaysia

*Author to whom correspondence should be addressed:
E-mail: ahmadsufian@uitm.edu.my

(Received January 31, 2023; Revised March 13, 2023; accepted March 20, 2023).

Abstract: Fibre metal laminate (FMLs) are hybrid composite materials which consisted of metallic layers and fibre-reinforced polymer. Currently, FMLs are becoming increasingly utilized in a wide range of applications, such as aircraft, automotive, marine, sporting goods and medical due to their specific mechanical properties like superior impact resistance and fatigue resistance. ARALL (Aramid-Reinforced Aluminium Laminate), which is based on aramid fibres, GLARE (Glass Reinforced Aluminium Laminate), which is based on high-strength glass fibres and CARALL (Carbon Reinforced Aluminium Laminate), which is based on carbon fibres, are the most commercial products FMLs. This article analyzes pertinent literature associated with experimental work on FMLs and their constituent materials subjected to impact loading. It reviewed the mechanical properties, impact performance indices, crushing behavior, failure modes, and failure mechanisms of various FML structures with different variables (impact energy, fibre orientation, layup configuration, stacking sequence, metal arrangement, direction and type of reinforcement, laminate thickness, metal thickness) under impact conditions (lateral and axial impacts). Overall, the literature on the response of FML flat plate structures to axial impact loads is unreported, and the most current research focusing on the axial crushing of FML tubes. Hence, further studies are required to increase the applicability of FMLs in applications that may be impacted under axial loading.

Keywords: axial impact loading; experimental; fibre metal laminate (FML); impact response; mechanical properties

1. Introduction

Composite materials and metallic alloys have seen widespread usage in a variety of specialty areas, particularly in the structural components of aircraft and automotive over the past few decades[1–5]. After World War II, the commercial use of composites was spurred by the successful use of these materials for military applications in the aircraft industry[6]. Composite materials provided significantly to the structural industry's weight reduction and offered numerous advantages over metallic alloys, such as the excellent ratio of strength-to-weight, great durability, lightweight, superior fatigue properties, better energy absorption and resistance to corrosion, wear, impact and fire[3,4,7–10]. However, composite materials and metallic alloys have disadvantages that limit their applicability, like poor fracture toughness and high moisture absorption of composites and fatigue failure of metallic structures[1,6,11,12]. Fibre metal laminate, often known as FML, was developed to address the challenges presented by both of these materials[1]. The FML is a hybrid composite structure comprised of metal and fibre-reinforced composite layers[13–17]. Fokker Aerostructures of the Netherlands attempted for the first time in 1950 to improve fatigue resistance by employing laminated materials[1,18]. Consequently, the performance of laminated materials was superior to that of composite and monolithic aluminium. This hybrid material combines beneficial metal and composite properties[15,19]. Thus, FML possesses both metal and composite properties.

Metal is an isotropic material whose properties are independent of direction. Meanwhile, composites and FML are anisotropic materials whose properties vary in all directions[20]. For instance, when the fibre lamina in a composite laminate are stacked in different directions, the properties will vary with the direction. The elastic modulus and ultimate strength are the two properties that have the most influence on the impact performance of a

material structure[20]. These two properties can be determined using Rules of Mixture (ROM) in terms of volume fraction of composite laminate and metal alloy[21]. Equations (1) to (3) are used to determine the elastic modulus and ultimate strength of the composite. $E_{1,c}$ is the longitudinal elastic modulus of the composite, whereas E_f and E_m are the fibre and matrix elastic modulus, respectively. V_f and V_m are fibre and matrix volume fractions, respectively. In Equation (2), σ_c is the strength of the material with the additional subscripts used analogously to their use in Equation (1). $E_{2,c}$ is the transverse elastic modulus of the composite, as shown in Equation (3).

$$E_{1,c} = V_f E_f + V_m E_m \tag{1}$$

$$\sigma_c = V_f \sigma_f + V_m \sigma_m \tag{2}$$

$$E_{2,c} = \frac{E_f E_m}{V_f E_m + V_m E_f} \tag{3}$$

Equations (4) to (6) are the analytical prediction for FML. MVF is defined as the ratio of the sum of the individual metal thicknesses to the total laminate thickness, as stated in Equation (6).

$$E_{FML} = MVF.E_m + (1 - MVF)E_c \tag{4}$$

$$\sigma_{FML} = MVF.\sigma_m + (1 - MVF)\sigma_c \tag{5}$$

$$MVF = \frac{\sum_1^n t_m}{t_{lam}} \tag{6}$$

t_m represents the thickness of individual metal layers, n represents the number of the metal layer, and t_{lam} is the thickness of the laminate.

1.1 Classification of FML

FMLs can be classified based on their structural configurations or material components. The FML's structural arrangements can be asymmetric, sandwich and multi-stacking laminates, dependent on performance and manufacturing needs[1]. Particularly for multi-stacking laminates, it is possible to generate specialized performance characteristics by alternating the stacking order and fibre orientations[1]. Laminate and reinforcement layup in FML can be written as (m/n) wherein m denotes the number of metal layers, while n represents the number of composite layers. This rule is only applicable for sandwiched or symmetric FML. For instance, 2/1 laminate (one reinforcement layer sandwiched between two metal layers) and 3/2 laminate (three metal layers separated by two reinforcement layers)[19].

It is permissible to classify FMLs based on their material constituents (metal and reinforcement), but there are other constraints to consider while constructing a reliable FML such as the availability and cost of materials constituents[1]. FMLs can be classed in various metal-based like aluminium (Al), steel, magnesium and titanium[1,14,16,17,22–25]. Aluminium-based FMLs such as ARALL, CARALL and GLARE which are reinforced with aramid fibre, carbon fibre and glass fibre are the most researched and developed because Al is the most widely used structural material in the current aviation industry[1,14,16,26].

ARALL is the first development of FML, created in 1978 at Delft University of Technology's Laboratory of Structures and Materials of Aerospace Engineering Faculty[16,17,22,23,27,28]. However, ARALL has low fibre-to-adhesive contact strength, resulting in poor peel strength and inter-laminar shear characteristics[26]. GLARE was then created in 1989 due to its high compressive strength and excellent adhesion between glass fibres and adhesive, despite the fact that aramid-epoxy composites have high specific strength, specific modulus, and impact resistance[6]. GLARE was commercialized on the Airbus A380, resulting in significant weight savings and exceptional wear and damage resistance[1,29]. More research was done using different material constituents to improve the mechanical characteristics of ARALL and GLARE. This led to the creation of CARALL around 1989[1,23]. Zhen[26] reported that CARALL suffers fatigue issues during flight simulation fatigue tests at extreme stress levels.

ARALL1 and GLARE1 are the FMLs that are most readily available for commercial use[14]. It was discovered that aramid fibre composites demonstrate greater low-cycle fatigue performance but worse high-cycle fatigue performance compared to carbon fibre composites. Combining high strength and stiffness with a superior impact property provides CARALL with a substantial advantage for use in space applications[4,6]. However, the FML's strength and stiffness can be altered by altering the stacking sequence of the metal and fibre in composite materials.

In addition, the direction of reinforcement can be classified into several categories, including unidirectional (UD), cross-ply (bi-directional)/woven laminates, and chopped strand mat[1]. The arrangement and orientation of fibres determine the characteristics and structural behavior of composite materials[8]. In the case of UD laminate, the fibre orientation will be either 0° or 90°. In the cross-ply laminate, the fibre will be twined in a manner that is analogous to the formation of textile fabrics. Cross-ply laminate beats UD laminate in terms of impact resistance and damage resistance, based on lateral impact studies[30]. Zhu and Chai[31] discovered that FML with UD fibres can resist a greater load with a bigger plastic zone compared to woven fibres with more localized deformation. According to Bienias et al.[12], the higher

failure strength and stiffness of UD fibres increase their impact resistance. This is because, in cross-ply, half of the fibres are arranged at 90˚.

1.2 Advantages and disadvantages of FMLs

FML possessed significant benefits over monolithic metal or fibre-reinforced composite due to the combination of the excellent characteristics of metals and fibre-reinforced composite. In addition to its benefits, FMLs also have some drawbacks. Table 1 shows the advantages and disadvantages of FMLs.

Table 1. Advantages and disadvantages of FMLs.

Advantages	
High strength	Metal and fibre-reinforced composites are extremely hard and inflexible, resulting in high stiffness[12,32].
Lower density	Provides a lightweight structural material[23,32,33].
Excellent corrosion resistance	The polymer in FML provides super corrosion resistance[12,23,26].
Excellent moisture resistance	Metal layers serve as barriers at the outer surface to slow the moisture absorption in FML than in polymer composite[1].
High fatigue resistance	Intact bridging fibres constrained the opening of fracture or fibre bridging properties[1,12,23,32,34,35].
High impact resistance	FML offers good impact resistance under impact loading in comparison to composite and monolithic metals. FML laminate can prevent the spread of Al fractures[12,15,23,26,32,36].
Fire resistance	Inflammability-sensitive parts are suitable. Fire cannot penetrate FML's interior layers because of its high fibre (glass fibre) melting point[1,12,22,37].
High capacity for energy-absorbing	FMLs have a high energy absorption capacity due to localized fibre breakage and shear failure inside the metallic plies[32,38,39].
Repairable of the damaged area	The scratched region can be repaired with riveted patches made of Al[23].
Disadvantages	
Long processing time	Intensive matrix curing processes in composite plies lengthen production cycles and reduce productivity[14]. Forming fault-free FML components with complex forms in high quantities remains a challenge[1].
High maintenance	The inhomogeneous through-thickness features of FMLs complicate quality inspection during manufacture and in-service maintenance[1].
Manufacturability	Despite advances in FML forming methods since the 2000s, there are still hurdles in manufacturability[1].
High cost	Cost of labor and FMLs as a whole increase[14]. Long processing cycle time increases the cost of labor and overall FMLs.

1.3 Application of FMLs

The above-mentioned benefits of FMLs have led to their widespread use in a variety of industries, with aerospace being one of the most prominent. Numerous aeronautical manufacturers, including Beech Starship, Deutsche Aerospace-Airbus, Cessna, Bombardier Aerospace, Aerospatiale, NASA, Garuda, US Airways, Air Canada, Lockheed, and EMBRAER, are interested in replacing traditional aluminium components with FML composites [6,40]. Fig. 1 presents the application of FML in aircraft components[1,23,24,40].

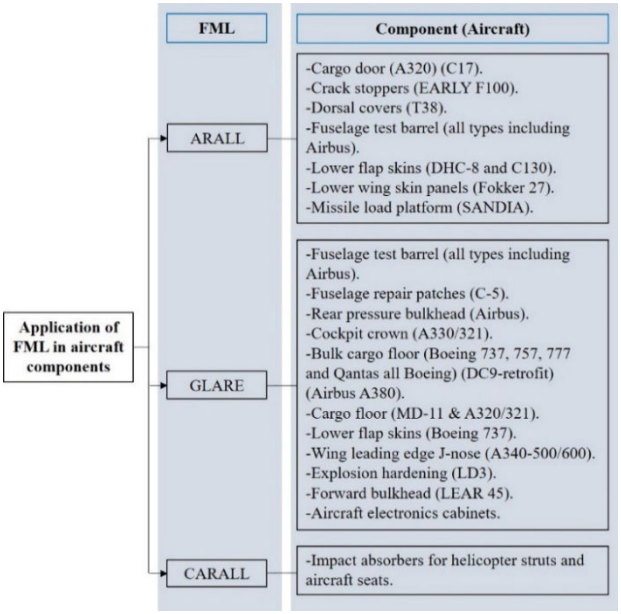

Fig. 1: Application of FMLs in aircraft components.

FMLs are also utilized to construct the front hood of cars to reduce vehicle weight and improve vehicle performance[24,32,41–43]. Moreover, FMLs can also be found in bicycle wheels, fishing rods, tennis and racquetball rackets, ice hockey sticks, ski poles, and surfboards because of their higher strength and stiffness and lower weight[43]. FMLs were utilized for marine applications such as propellers and hulls due to their superior water absorption and good corrosion resistance[8,43,44]. There is a high probability that these applications may be exposed to various types of loading, including impact loading.

2. Mechanical properties and impact behavior of FML and its constituents

Nowadays, FMLs are widely utilized in many applications and they are easily exposed to a variety of loadings especially impact loading. This paper primarily aims to discuss further the impact response of FML and its constituents subjected to impact loading. In general, the impact condition or reaction can be separated into two categories: lateral impact and axial impact. The impact that occurs parallel to the thickness of the laminate is lateral. Meanwhile, the axial impact is the impact that happens in the direction of the laminate's length[45]. The impact performance of FML and its constituents can be evaluated based on several indicators, including energy absorption (EA), specific energy absorption (SEA), mean crushing force (F_{mean}), peak crushing force (PCF) or peak load (P_{max}) and crush force efficiency (CFE). These performance indicators can be derived directly from the force-displacement curves[46]. The EA refers to the overall energy absorbed by the structure during the crushing process, as calculated by the area under the force-displacement curve, as shown in Equation (7).

$$EA = \int_0^d F(x)dx \qquad (7)$$

F(x) represents the crushing load and *d* is the relevant crushing distance. The greater a structure's EA, the greater its capability to absorb energy[46]. The SEA is a measure of the energy absorbed by the mass of the structure, as shown in Equation (8).

$$SEA = \frac{EA}{m} \qquad (8)$$

m is the structure's mass. The greater the SEA, the greater the material usage efficiency for the structure's energy-absorption. The F_{mean} is the mean impact force experienced by a structure, as determined by Equation (9).

$$F_{mean} = \frac{EA}{d} \qquad (9)$$

d is the distance of impact. The greater the F_{mean}, the greater the capability of the structure to absorb energy when deformed. The PCF represents the maximum impact loading load. Equation 10 defines the CFE as the ratio of the F_{mean} to the PCF. The greater the CFE, the better performance of the energy absorbing structure.

$$CFE = \frac{F_{mean}}{PCF} \qquad (10)$$

Research on the experimental axial impact test of FML is significantly limited. Hence, the impact response of FMLs under lateral impact loading will be discussed as well to obtain an overview of the impact response on FML structure.

2.1 Impact test on FMLs

The FML is intended to improve the performance of the composite structure under a variety of impact-loading conditions. The purpose of the impact test is to evaluate the mechanical properties and resistance to failure of FMLs when subjected to forces such as collision, a falling object, or a sudden blow. Many researchers have carried out lateral impact tests on FML structures.

Hozumi et al.[38] investigated the response to three different impact energy levels for GFRP-AL FMLs with woven and unidirectional (UD) glass fibre reinforcement and an Al sheet in the middle. Both the woven and the UD types yielded nearly identical results in terms of the FML energy absorbed as shown in Fig. 2.

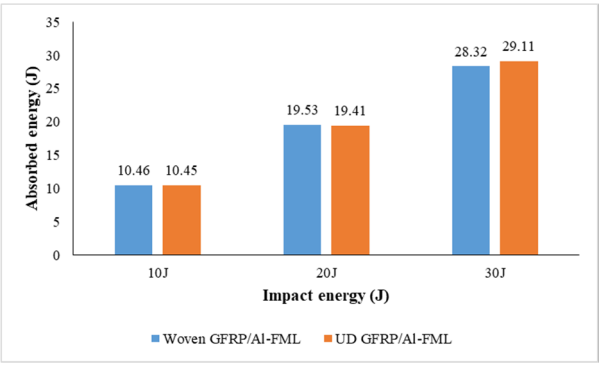

Fig. 2. Energy absorbed by woven GFRP/Al-FML and UD GFRP/Al-FML[38].

Inadequate adhesion between the GFRP and Al sheet caused them to become separated and delaminated when an impact load was applied. Due to inefficient bridging between them, the GFRP-AL FML absorbed less energy. Consequently, the absorbed energy by GFRP-AL FML was similar to GFRP with UD-type glass fibre. The results produced by Trzepiecinski et al.[47] also supported this conclusion. The optical study showed that the impact loading led to the de-bonding of the GFRP-AL, fibre breaking, fibre delamination, and matrix cracking. As the impact energy was prolonged, the specimen deflected farther for all GFRP and GFRP-AL FML composites. Fibre-matrix and GFRP-Al de-bonding occurred during the impact test, hence placing the GFRP at the outer layers of the FML systems did not increase the impact resistance[38]. Jakubczak et al.[48] discovered that the absorbed energy of metal-fibre hybrid titanium-carbon composite laminates (HTCL) increased when the impact energy increased. Lokesh et al.[49] investigated the impact behavior of Al-Kevlar fabric/epoxy FML with a constant mass at three different impact velocities; (5m/s=48.91J, 6m/s=70.2J, 7m/s=95.55J). Results revealed that the FML

can withstand the maximum impact energy of 70.2J. Meanwhile, Zhu and Chai[31] examined the impact dynamic response and failure modes of 2/1-GLARE which is made up of two different types of glass fibre-reinforced plastics: unidirectional (UD) and woven. According to the results, FML with UD fibres (specimen C2 and C4) exhibited superior impact resistance than FML with woven fibres, since their peak load and energy to failure were higher. This was frequently strengthened by the higher stiffness and failure strength of UD fibres. The sanding of the adhesive faces of the Al layers slightly improved specimen C4's impact resistance, resulting in a higher peak load than that of specimen C2, as shown in Table 2. Moreover, Table 2 indicated that the impact resistance of FMLs with woven laminate (specimen C5 and C6) was not significantly affected by increasing the glass fibre-reinforced layer thickness. The perforation hole in FML with woven fibres was about a square, but the perforation hole in FML with unidirectional fibres was nearly a straight-line crack. This was because FML with UD laminate absorbed significant impact energy and caused the FML with woven laminate suffered perforation. As the contact force increased, the plastic area in the Al layer expanded from the point of contact toward the boundary[31].

Table 2. Peak load and failure energy of FMLs (woven and UD)[31].

FML	Thickness (mm)	Failure energy (J)	Peak load (kN)
C1-Woven (No sanding)	0.970	12.10	2.496
C2-UD (No sanding)	0.973	13.48	3.024
C3-Woven (Sanding)	0.964	12.13	2.576
C4-UD (Sanding)	1.085	13.44	3.148
C5-Woven (Sanding)	1.178	12.06	2.477
C6-Woven (Sanding)	1.022	12.02	2.392
C7-Woven (Sanding)	0.913	11.80	2.473

Yaghoubi et al.[50] tested glass-reinforced (GLARE) 5 FML specimens of varying thicknesses (2/1, 3/2 and 4/3) using a drop-weight impact tester to determine the impact response and damage caused by the impactor mass. They explained that the failure mode varied depending on the material thickness and impactor mass. The thicker plies of GLARE 5 provided greater resistance to impact. It was found that a greater amount of energy was absorbed, the overall damaged contour expanded and the maximum local deflection decreased with increasing specimen thickness. For GLARE laminates, the size of internal damage size was never as large as the visible plastic deformation exhibited on the external Al layers. Reducing the impactor's mass while keeping the impact energy constant led to a larger permanent local deflection. As a result, the panel subjected to the lighter impactor mass would reach the perforation limit more quickly than the panels treated to a larger impactor mass. Besides that, the contact force also increased and the damage pattern changed. They concluded that panel thickness influenced the essential behaviors of GLARE 5 FML specimens. This observation tallied with the results obtained by Rakham and Giridharan[39], who found that the GLARE laminate absorbed significantly more energy than the GFRP laminate and experienced significantly less deformation than GFRP laminate due to the reinforcement provided by Al sheets. They concluded that the energy absorbed increased with the number of layers. Due to the incorporation of an Al sheet, GLARE laminates demonstrated superior impact strength and stiffness compared to GFRP laminates, despite having the same overall thickness. The peak load of GLARE laminate was greater than that of GFRP laminate[39].

Sivakumar et al.[33] studied the Charpy impact response of Kenaf (K)/glass (G) fibre-reinforced Al 5052 laminates (FMLs) with various stacking configurations (GGG, GKG, KGK, KKK) and orientations (0˚/90˚ and ±45˚). The composite laminate was sandwiched by two layers of Al layers. The impact strength of FMLs in an edgewise direction was greater than that FMLs in a flatwise direction. This was due to the greater energy required for fracture initiation of FMLs in the two different fibre orientations. Both in the flatwise and edgewise directions, GKG FMLs with 0˚/90˚ and ±45˚ fibre orientations had the highest impact strength, while KKK FMLs exhibited the lowest. The substitution of glass fibre at the outer layers of hybrid composite resulted in higher impact strength. Glass fibre has greater impact resistance than Kenaf fibre. However, the placement of kenaf fibres in the outer layers of hybrid composites decreased the impact resistance because fibre-matrix de-bonding occurred when the outer kenaf layer broke, and the bridging mechanism between kenaf fibre and glass fibre was therefore less effective. In addition, kenaf fibres have a poorer impact resistance in comparison to glass fibres. It was established that the addition of a small amount of Kenaf fibres to hybrid composites improved their resistance to impact. This was likely owing to the enhanced bonding capacity of kenaf fibres, which increased impact strength. According to Sivakumar et al.[33], the impact properties of the laminates were affected by the fibre-matrix adhesion.

Sathyaseelan et al.[51] conducted the Izod impact test on the CARALL FML in two distinct orientations and stacking sequences as shown in Table 3 to establish the FML's mechanical properties. Vasumathi and Murali[16] also conducted an Izod test on CAJRALL (CArbon-Jute Reinforced ALuminium Laminate) FMLs and CAJRMAL

(Carbon-Jute Reinforced MAgnesium Laminate) with two different stacking sequences as illustrated in Table 3.

Table 3. Stacking sequences of CARALL, CAJRALL and CAJRMAL FMLs[16].

FMLs	Stacking order	Stacking sequence
CAJRALL	1	(Ca_0°/Al/Ca_{45}°/Al/Ju_0°/Ju_{90}°/Al/Ca_{-45}°/Al/Ca_0°/Al/Ca_{-45}°/Al/Ju_0°/Ju_{90}°/Al/Ca_{-45}°)
	2	(Ca_0°/Al/Ca_{90}°/Al/Ju_0°/Ju_{90}°/Al/Ca_{90}°/Al/Ca_0°/Al/Ca_{90}°/Al/Ju_0°/Ju_{90}°/Al/Ca_{90}°/Al)
CAJRMAL	3	(Ca_0°/Mg/Ca_{45}°/Mg/Ju_0°/Ju_{90}°/Mg/Ca_{-45}°/Mg/Ca_0°/Mg/Ca_{-45}°/Mg/Ju_0°/Ju_{90}°/Mg/Ca_{-45}°)
	4	(Ca_0°/Mg/Ca_{90}°/Mg/Ju_0°/Ju_{90}°/Mg/Ca_{90}°/Mg/Ca_0°/Mg/Ca_{90}°/Mg/Ju_0°/Ju_{90}°/Mg/Ca_{90}°/Mg)
CARALL	5	($Ca_{0'}$/Al/$Ca_{90'}$/Al/$Ca_{0'}$/$Ca_{90'}$/Al/$Ca_{90'}$/Al/$Ca_{0'}$/Al/$Ca_{90'}$/Al/$Ca_{0'}$/$Ca_{90'}$/Al/$Ca_{90'}$/Al)
	6	($Ca_{0'}$/Al/$Ca_{45'}$/Al/$Ca_{0'}$/$Ca_{90'}$/Al/$Ca_{-45'}$/Al/ $Ca_{0'}$/Al/$Ca_{45'}$/Al/$Ca_{0'}$/$Ca_{90'}$/Al/$Ca_{-45'}$/Al)

The difference between stacking orders 5 and 6 and stacking orders 1 and 2 was that the 90˚ layer at the non-cross-ply layer was replaced by 45˚. The results demonstrated that the impact resistances of stacking orders 6 and 1 were larger than that of stacking orders 5 and 2, respectively. CAJRALL specimens had a greater impact toughness than CAJRMAL ones. The arrangement of carbon fibres at 45˚ orientation can sustain shear force better than the 90˚ orientation. Consequently, the stacking order and fibre orientation significantly affected the performance of FML specimens. Hozumi et al.[38] reported that there was no advantage by putting composite laminate at the outermost layer.

Sharma et al.[52] studied the effect of Al layer distribution on four distinct layup configurations of FMLs (GLARE) with varying sheet thicknesses of Al alloy (2/1-0.6, 3/2-0.4, 3/2-0.3(O), and 4/3-0.3). 3/2-0.3(O) denotes three Al layers, two composite layers, and two Al layers were 0.3 mm thick on the outside and one Al layer was 0.6 mm thick on the inside, meanwhile, 3/2-0.4 denotes three Al layers, each with a thickness of 0.4 mm, and two composite layers. The metallic layers have been positioned in different locations while keeping the total thickness of the metal layer constant. The total thickness of FML was different. The low-velocity impact (LVI) test was conducted at five different impact energy levels. The results indicated that FML 2/1-0.6 exhibited less cracking and deformation because the composite layers were stacked together. A similar result was obtained by Khan et al.[53]. Meanwhile, FML 4/3-0.3 exhibited the highest cracking and deformation because two adjacent composite layers with distinct fibre orientations were separated by metallic layers. The deformation was caused by the distortion of the Al layer. FML 4/3-0.3 absorbed the highest energy and the FML 2/1-0.6 absorbed the lowest energy at all energy levels. The dent creation was observed close to the location of impact due to the plastic deformation of the top and bottom layers of Al, which led to the absorption of energy. This observation was similar to the results obtained in the studies of Rakham and Giridharan[39] and Yaghoubi et al.[50]. The size of the dent grew as the energy of the impact increased[52,54]. All FMLs exhibited delamination between the adjacent Al layer and the composite layer[52,54]. Ramadhan et al.[55] studied the impact response of FML based on Kevlar-29 fibre/epoxy-Alumina resin with different stacking sequences of Al 6061-T6 plates. The FML with the front and middle Al stacking sequences were tested at thicknesses of 4mm, 8mm, 12mm, 16mm and 20mm, meanwhile the FML with the back Al stacking sequence was tested at thicknesses of 4mm, 8mm, 12mm, 16mm, 20mm and 24mm. The energy absorption of all specimens increased as the thickness increased. The energy absorption of FML with the back Al stacking sequence was the highest. The FML with a front stacking sequence experienced the most critical case as it had the lowest energy absorption. The overall results obtained by the Al back stacking sequence plate were the optimum structure to resist the impact loading, as can be seen in Fig. 3.

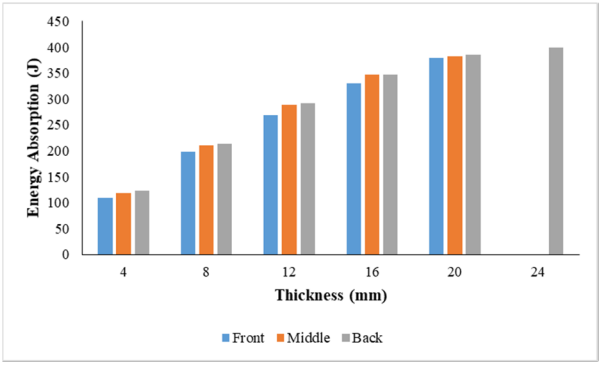

Fig. 3. Comparison of the front, middle and back Al stacking sequence on the energy absorption versus specimen thickness of Kevlar-29/epoxy-Al_2O_3/Al alloy[55].

Moriniere et al.[56] reported that GLARE 5-2/1-0.4 absorbed 30% more impact energy than GLARE 5-2/1-0.3, with 90% of the energy dissipated by the Al layers, as can be seen in Table 4. The same trend was found between GLARE 5-3/2-0.4 and GLARE 5-3/2-0.5 as shown in Fig. 4[57]. It can be concluded that the thickness of the metal and the arrangement of the layup could affect the impact

resistance of FML[52].

Table 4. Test results for GLARE 5-2/1-0.3, GLARE 5-2/1-0.4, GLARE 5-3/2-0.4 and GLARE 5-3/2-0.5[56,57].

References	56)		57)	
	GLARE 5-2/1-0.3	**GLARE 5-2/1-0.4**	**GLARE 5-3/2-0.4**	**GLARE 5-3/2-0.5**
Maximum force (kN)	3.87	4.01	8.00	8.37
Maximum displacement (mm)	11.26	11.54	3.16	2.55
Energy absorption (J)	14.63	19.05	N/A	N/A
Specific energy absorption (J m^2/kg)	5.53	5.95	N/A	N/A

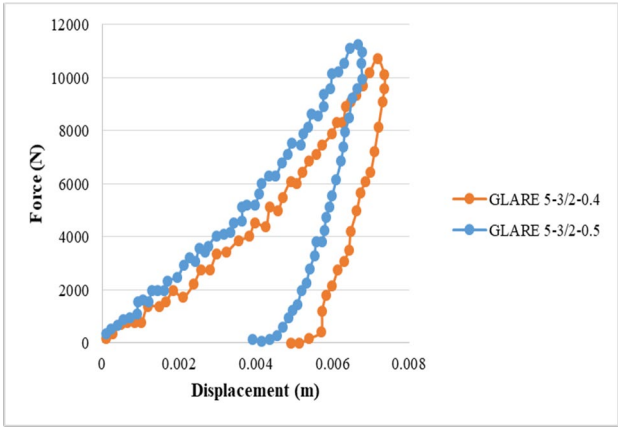

Fig. 4. Force versus displacement of GLARE 5-3/2-0.4 and GLARE 5-3/2-0.5[57].

Starikov[58] reported that the area of impact delamination observed in HSS (High Static Strength) GLARE specimens was greater than that found in Standard GLARE specimens. However, the Standard GLARE laminates revealed deeper dents than HSS GLARE laminates due to the superior impact resistance and potential influence on aircraft operability of Standard GLARE. He concluded that the mechanical characteristics of the alloy used in GLARE significantly influenced the impact behaviour of GLARE laminates.

Fan et al.[59] performed the LVI test on three different layup configurations ((2/1), (3/2), (4/3)) of GLARE with three different numbers of woven glass fibre prepreg plies (4, 8 and 16). The test aimed to investigate the perforation resistance and responsiveness of GLARE by varying the target thickness, projectile diameter, and impact radius and comparing the findings to three different plain composite laminates on which the FMLs were based. The FMLs exhibited greater resistance to perforation and absorbed significant energy than their plain composite counterparts, as shown in Fig. 5 and Fig. 6, respectively. By examining cross-sectional samples, failure mechanisms such as fibre fracture, metal layers fracture, composite and metal layers delamination, and plastic deformation in the Al plies were identified. FMLs were thicker and stiffer than composites, which resulted in a higher peak load during impact. The amount of energy necessary to perforate the target increased with target size, plate thickness (number of metal and composite layers in the FML) and indenter diameter. Subsequently, the perforation resistance of FML increased. This was a result of FML's ability to absorb energy during elastic and, more significantly, severe plastic deformation. Changes to the impact location (corner or along the target's edge) did not affect the perforation response and impact resistance of the target. Overall, FMLs exhibited higher resistance to perforation than composites.

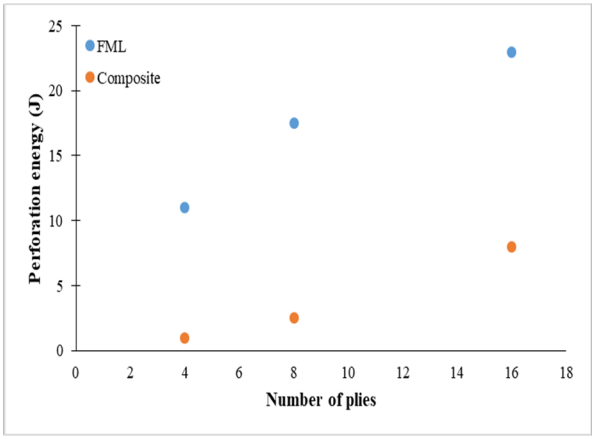

Fig. 5. Perforation energy of the composites and 2/1 (4-plies, 8-plies and 16-plies) FMLs subjected to LVI testing[59].

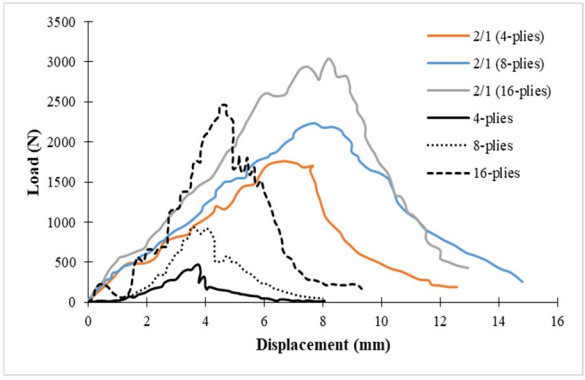

Fig. 6. Load versus displacement of the composites and 2/1 (4-plies, 8-plies and 16-plies) FMLs subjected to LVI testing[59].

Wu et al.[60] examined the impact performance of cross-ply S2-glass fibre prepreg-reinforced Al laminates (GLARE5-2/1 and GLARE4-3/2) and compared it to the Al 2024-T3, which served as a baseline material. According to the results, both GLARE laminates offered superior resistance to impact damage than the Al 2024-T3.

GLARE 5-2/1 exhibited greater impact resistance than GLARE 4-3/2. This was because the composite laminate was stacked together as reported by Sharma et al.[52]. In comparison to GLARE4-3/2 laminate and Al, GLARE5-2/1 laminate required more specific energy to cause a noticeable crack in the outer layer of Al on the side that was not affected by the impact. The amount of energy required to perforate the GLARE 4-3/2 was the highest due to the excessive number of metal and composite layers in FML. This result was similar to Fan et al.[59]. Both GLARE laminates had a higher specific perforation energy than Al and GLARE 5-2/1 possessing the highest value. Fig. 7 indicated the perforation energy and specific perforation energy of GLARE 5-2/1, GLARE 4-3/2 and Al. Due to bending deformation, the initial failure of GLARE laminates was observed as a noticeable fracture in the outer Al layer on the side that was not impacted. The Al layer's impacted side failed as the impact energy increased, and as it kept rising, a through-crack was formed[60]. The size of damage for both GLARE laminates increased when impact energy increased and the result was equivalent to Sharma et al.[52].

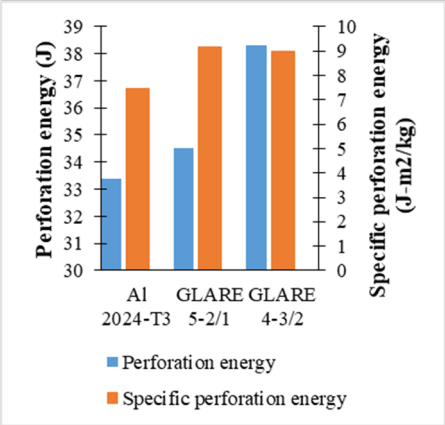

Fig. 7. Perforation energy and specific perforation energy of Al 2024-T3, GLARE 5-2/1 and GLARE 4-3/2[60].

Melba and Kumar[61] investigated the impact response and damage tolerance of woven fibre mats based-GLARE and chopped strand mats (CSM) GLARE. Al sheet of the same thickness as the GLAREs was utilized to compare the results. The woven-based GLARE resisted a higher impact load and absorbed 3.4% higher energy than the CSM-based GLARE. The woven-based GLARE showed superior impact response and damage resistance with minimal deformation compared to the CSM-based GLARE and Al sheets. The elasticity of woven-based GLARE led to less permanent deformation[61]. Continuous fibres in woven-based GLARE with high strength and modulus permitted more energy absorption than discontinuous fibres in CSM-based GLARE. The lower strength of the discontinuous fibres contributed to the poor impact response of CSM-based GLARE[20,62]. The damaged area and penetration depth of woven-based GLARE were considerably less than those of CSM-based GLARE and Al sheets[61].

Romli et al.[63] conducted a quasi-static impact test to examine the failure behavior of the 2/1 Al/CFRP laminate FML at five different crosshead displacement rates: 1mm/min, 5mm/min, 10mm/min, 50mm/min, and 100mm/min. As the crosshead displacement rate of the FML increased, the damage surface area of the FML also increased. The failure modes that occurred in FML included delamination between the composite layer and delamination at the metal-composite interface, fibre failure, plastic deformation and cracking of the Al layer. Increased crosshead displacement rate resulted in less deterioration of the composite structure and increased the strength of FML. Lower crosshead displacement rate led to severe delamination of the middle component and base ply. The authors concluded that the failure was dependent on the ductility of the Al.

Yaghoubi and Liaw[64] conducted a ballistic impact test on the GLARE 5 beam by varying the thickness (layup configuration from (2/1) to (6/5)) and stacking sequence (cross-ply [0˚/90˚]s, unidirectional [0˚$_4$], unidirectional [90˚$_4$], quasi-isotropic [0˚/±45˚/90˚]. The unidirectional [90˚]$_4$ specimen exhibited the least resistance to projectile perforation, according to the data. With the exception of the unidirectional [90˚$_4$] specimen, the ballistic limit was almost constant with the stacking sequence. As the thickness of the panel increased by modifying the specimen configuration from (2/1) to (6/5), the ballistic limit also increased. Taheri-Behrooz et al.[65] investigated the influence of stacking sequence on the impact response of Al-glass/epoxy FMLs, and their findings highlighted that the [Al/(±45)$_8$/Al] lay-up sequence had a higher load-carrying capacity than the other lay-ups. Reyes Villanueva and Cantwell[66] utilized a nitrogen gun to conduct the high-velocity impact (HVI) test on the FMLs sandwich structures which comprised of glass fibre-reinforced polypropylene (GFPP) prepreg (UD and woven) with Al 2024-T3. The results showed that the UD FML appeared to have superior energy-absorption capabilities than the woven FML sandwich structure through failure mechanisms like fibre-matrix de-bonding, longitudinal splitting, and Al cracking. Increasing the impact energy caused the Al and composite layers in the bottommost FML skin to crack. The UD FML systems have 7.5% of perforation energy and 9% of specific perforation energy higher than the woven FML sandwich structures. The specific perforation energy of the FML sandwich structures (both UD and woven) was greater than that of Al, as shown in Fig. 8. This was due to the fact that thermoplastic composites had a higher impact resistance than Al. The better impact response of FML compared to the Al was attributable to energy-absorbing mechanisms including plastic deformation in the thin Al plies and matrix cracking and fibre fracture in the composite layers[66].

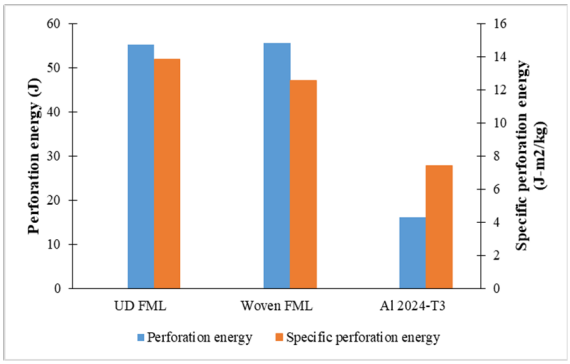

Fig. 8. Perforation energy and specific perforation energy of UD FML, woven FML and Al 2024-T3[66].

In conclusion, FMLs were subjected to various impact loading including LVI[39,50–57,59], HVI[66], quasi-static impact[63], ballistic impact[64], Charpy impact[33] and Izod impact[16,51] tests. The FMLs had superior impact properties compared to composite and metal alloys (which act as baseline material)[60]. The energy absorption of FML was influenced by the direction of reinforcement[31,38,47,61] and adhesion strength between composite laminate and metal layers[31,38,47]. FML with UD fibre exhibited superior impact resistance compared to woven-based FML[31,66], meanwhile woven based FML had good impact resistance than chopped strand mat-based FML[61]. The type of reinforcement and fibre orientation/stacking sequence of fibre ply affected the impact performance of the FML structure[33,38,63,65]. Impact resistance of FMLs can be affected by metal arrangement in FML structure[38,52,53,64] but not significantly affected by the thickness of composite laminate[31,55]. However, increasing the thickness of the FML structure or the number of layers in the FML structure increased the impact resistance and energy absorption of FML[39,50,59,64]. Then, less deformation would occur in FML compared to composite laminate due to the reinforcement provided by Al sheet[39,52]. The deformation of FML as well as the energy absorption was dependent on the thickness of metal layers[52,56,57]. This was because the MVF influenced the peak load, deflection at peak load, EA and SEA of the structure[48,67,68]. Nevertheless, sandwiched composite laminate with 2/1 layup configuration had better impact resistance and exhibited less deformation or cracking than 3/2 and 4/3 layup because the composite laminates were continuously stacked together[52,60].

2.2 Impact test on composite

Investigating the mechanical properties of composite materials under impact loading is necessary as composite is a constituent material of FMLs. The mechanical properties of composite primarily influenced the impact characteristic and response of FML structure when subjected to impact loading. Moreover, the composites were utilized extensively in the aircraft industry during World War II before the development of FMLs due to their high strength, high stiffness, high fatigue resistance, and high corrosion resistance. Hence, many researchers conducted impact tests on composite materials and compared the results with FML structures and metals. When subjected to impact load, the composite materials performed poorly in comparison to metal alloys[23].

Guades et al.[69] conducted the repeated axial impacts on nine-ply square fibre-reinforced polymer (FRP) composite tubes to determine their behaviors. The effects of impactor mass, incident energy (by maintaining or altering the impactor mass or drop heights) and the number of impacts were investigated. When the E630 was hit 45 times and the E480 and E420 were hit 130 times, the composite tubes impacted by higher incident energies collapsed. When the number of impacts was low, the incident energy was a significant influence in the collapse of the tubes. Up to 130 impacts with lower incident energies, the composite tubes didn't show any visible damage, but internal damage (referred to as barely visible impact damage) may have happened. The fibre composite material's strength degraded due to the existence of internal damage. This indicated that the number of impacts became the most influential concern when the incident energy dropped. At lower incident energies, the impactor's mass had a notable effect on the collapse of tubes, but, at higher energies, its effect steadily reduced. At higher incident energies (E420, E480, E630), the peak load primarily dropped until the beginning of collapse (pre-collapse) and then remained unchanged in the post-collapse region. At lower incident energies (E160, E210, E320), the peak load dropped as the number of impacts increased. When the collapsed tubes were impacted with higher incident energy, their peak load degraded more quickly. At higher incident energies, rebound and end crushing were seen during the test. The 1st and 10th impacts caused the rebound case, however, the 30th and 40th impacts generated the final crushing case (all of the impact energy was absorbed by the composite tube). It has been demonstrated that incident energy effects and the number of impacts only have a significant impact on the rate of energy absorption in the pre-collapse region (Ist and 10th impacts), not in the post-collapse region.

Shaari et al.[70] investigated the impact behavior of four different types of composite laminate with varying Kevlar to glass fibre ratios (0:100, 20:80, 50:50 and 100:0). Results indicated that the addition of Kevlar fibre to glass fibre enhanced the composite laminates load carrying capability, energy absorption and degree of damage while slightly reducing deflection. These results demonstrated that Kevlar had superior impact resistance. Analysis of the damage pattern revealed that GFRP had a larger damage area than KFRP. As Kevlar fibre could absorb higher energy, hybridizing Kevlar fibre with glass fibre laminate tends to reduce the damaged area of the hybrid specimens. The percentage of fibre influenced the strength and behavior of the structure subjected to applied stress[3,9,71–74].

Hozumi et al.[38] investigated the influence of impact loading at three different energy levels (10J, 20J and 30J) on woven and UD glass fibre-reinforced composites (GFRP). The woven type of GFRP was thicker than the UD type because it had 20 plies of glass fibre as compared to 12 plies of glass fibres in the UD type. The woven type of GFRP had lower density and higher hardness than the UD type of GFRP. Results indicated that peak load and deflection increased as impact energy rose for both GFRPs. The UD type of GFRP had higher deflection than the woven type of GFRP. In contrast, the woven type of GFRP exhibited a higher peak load than the UD type of GFRP. Consequently, the UD type of GFRP showed higher energy absorbed compared to the woven type of GFRP at all impact energy levels. It can be concluded that the GFRP required greater deflection to absorb more energy and that energy absorption increased with increasing impact energy. When the impact energy increased, the damaged area also increased. Choong et al.[75] analyzed the impact behavior of woven GFRP composite at different impact energy levels (7.35J, 29.40J, 58.80J and 88.24J) with varying impactor drop height and a constant mass. They created a simple assumption of no energy losses and led to the energy absorbed being equivalent to the impactor potential energy. Table 5 presented the energy absorption of UD and woven GFRP composite when the input energy increased. Results revealed that the energy absorption increased as the impactor drop height increased. A similar result was found as the size of the damage zone consistently increased with the absorbed energy.

Table 5. Energy absorbed by UD GFRP and woven GFRP when the input energy increased[38,75].

Energy level	**Energy absorption**[38]		**Energy level**	**Energy absorption**[75]
	UD GFRP	**Woven GFRP**		**Woven GFRP**
10J	10.46±0.22	9.34±0.08	7.4J	7.4J
20J	20.19±0.68	16.63±0.73	29.40 J	29.40J
30J	29.63±0.35	23.69±0.61	58.9J	58.9J
-	-	-	88.3J	88.3J

According to Shaari et al.[70], the damage pattern served as an indicator for estimating the energy absorption in composite laminate via mechanisms including fibre breakage and delamination. The larger impact energy and larger damage area revealed that all types of GFRP laminates absorbed more energy. Evci and Gulgec[76] evaluated the impact properties of three different types of composites: UD E-glass, woven E- glass and woven aramid. Results demonstrated that woven fibre was more resistant to impact than UD fibre. This was because the fabric cells generated by the weft and warp yarns inhibited damage formation in the woven composites. Hence, development outside the cell zone was not possible. The impact resistance of Aramid fibre was also discovered to be superior to that of glass fibre. Yaakob et al.[44] determined the material properties of Aerohelmet made up of kenaf and flax materials subjected to drop-weight impact testing. Results indicated that Kenaf Aerohelmet had a better performance in absorbing energy with less deformation due to its strength even though the thickness of the Kenaf Aerohelmet shell was less than Flax Aerohelmet shell.

Srivastava[77] investigated the impact behavior of sandwich GFRP-polyurethane foam core-GFRP structure subjected to Izod impact, Charpy impact and weight drop impact conditions. Results indicated that the weight drop impact test exhibited the highest energy absorption. The upper and lower surfaces of the GFRP composites were entirely damaged during the Izod and Charpy impact tests. Due to the localized impact energy and specimen thickness, sandwich structures fractured from the impactor point as a result of the dominating flexural behaviours[76]. Notched specimens absorbed less energy compared to un-notched specimens. The only top face of the sandwich structure was fractured during the weight drop impact test because the impact energy was distributed consistently across the width of the specimen. Because the foam core absorbed the most energy, this demonstrated excellent mechanical resistance, preventing the creation and transition of cracks from the top face to the back face. Compared to Izod and weight drop impactors, the Charpy impactor showed high dynamic fracture toughness. The weight drop impact energy had the lowest dynamic fracture toughness than that of the Charpy and Izod impact tests. According to Bull and Edgren[78] research, this may come from vibrations of the supports and the initiation of material damage.

Fan et al.[59] performed the LVI test on 4-plies, 8-plies and 16-plies of 2/1 woven glass fibre prepreg composite to investigate the perforation resistance of composite laminate. The perforation energy increased when the composite plate thickness and indenter diameter increased. Rakham and Giridharan[39] also reported that the peak load and energy absorption increased when the number of fibre ply increased, as shown in Table 6. Maximum force and maximum deflection rose rapidly with increasing indenter size, demonstrating better energy absorption as indenter diameter increased. Similar perforation energy was observed regardless of impact locations or target size (corner, center, edge). It indicated that altering the impact locations had no significant influence on the perforation resistance of the target. The authors suggested a comprehensive investigation of this effect on larger structures[59].

Table 6. Energy absorption of composite with increasing the number of fibre ply[39].

[59]		[39]	
Number of plies	**Energy absorption**	**Number of plies**	**Energy absorption**
4	1	7	16.8
8	2.5	9	24.4
16	8	-	-

Reyes Villanueva and Cantwell[66] conducted the HVI test on the cross-ply and woven glass fibre-reinforced polypropylene (GFPP) composite laminate. Results illustrated that the cross-ply GFPP composite laminate absorbed more energy than the woven system. This occurred because the cross-ply GFPP composite laminate exhibited a variety of failure mechanisms like longitudinal splitting along the direction of the fibre, fibre fracture and delamination between the lowest composite plies. In contrast, the woven GFPP composite laminate had a significantly smaller delamination zone (local deformation and fibre failure) and inhibited longitudinal splitting along the fibre direction. Zhu et al.[79] reported similar results following an HVI test on a woven Kevlar/polyester laminate. The woven GFPP composite possessed 13% higher perforation energy than that of the cross-ply system. This may be partially attributable to the slightly thicker woven laminates (4.3 mm compared to 3.44 mm). The cross-ply laminates had almost 10% larger specific perforation energy than the woven ones. Probably due to the larger delamination area in the cross-ply laminates[66].

In conclusion, composite structures were subjected to various impact loading such as LVI[59], HVI[66,79], Izod impact, Charpy impact and weight drop impact tests[77]. The weight drop impact test exhibited the highest energy absorption and the lowest dynamic fracture toughness[77,78]. The drop height, number of impacts[69,75] and indenter size[59] were parameters that affected the energy absorption in the composite structure. The number of impacts and drop heights were directly proportional[69]. Hybridizing another fibre with another fibre composite laminate with a specified ratio improved the load-carrying capability and energy absorption of the composite. It would also reduce the damaged area of the composite compared to a composite with 100% of one fibre type only[70]. Besides, the peak load and deflection were dependent on the impact energy[38] and laminate thickness[39]. A greater deflection was required to absorb more energy[38]. Larger impact energy resulted in a larger damage area[38,70]. Moreover, the direction and type of reinforcement influenced the energy absorption, impact resistance and deformation of composite laminate[38,44,66,76]. For example, UD GFRP showed higher energy absorbed compared to woven GFRP at different impact energy levels[38]. The cross-ply GFRP composite laminate absorbed more energy than the woven system[66]. In the meantime, the woven fibre was more resistant to impact than UD fibre[76].

2.3 Impact test on metal

The impact test is performed on metals as well to investigate the impact resistance of metals. Typically, metal serves as a comparative baseline for FML or composite. In some instances, the FML has not yet been recognized or established. Consequently, metal is the most prevalent material utilized in numerous industries, including aircraft, marine, automobile, sports, construction, and medicine [5,25].

Wu et al.[60] examined the impact characteristics and damage tolerance of a monolithic Al alloy which served as a baseline material for comparison with GLARE (Al alloy and cross-ply S2-glass prepreg); GLARE 4-3/2 and GLARE 5-2/1 at various impact energy levels. Results showed that the Al alloy required the highest impact energy compared to GLARE laminates to create the first cracking. Similar research was conducted by Seo et al.[35], they reported that the Al 2024-T3 had a longer crack initiation life than GLARE when subjected to similar applied stress. It indicated that the Al 2024-T3 required the longest period or the most number of cycles for cracking initiation. According to Wu et al.[60], the specific perforation energy of Al alloy was lower than GLARE laminates. The dent depth of Al alloy was approximately the same as GLARE laminates but GLARE5-2/1 exhibited a slightly larger dent depth. The results demonstrated that the Al 2024-T3 had worse impact characteristics compared to the two GLARE laminates[59]. Reyes Villanueva and Cantwell[66] also demonstrated that the perforation energy of Al alloy was less than that of composites and GLAREs (woven and UD fibres). A similar study was conducted by Melba and Kumar[61] to determine the impact response and damage resistance of the Al sheet for comparison with glass fibre epoxy-aluminium metal laminates, GEAML (woven and chopped strand mats). Results revealed that the Al sheet had poor energy absorption and a larger damage area than woven-based GLARE but the Al sheet had better energy absorption and a smaller damage area than CSM-based GLARE. The perforation energy of metal exhibited from the test conducted by Wu et al.[60], Reyes Villanueva and Cantwell[66] and Melba and Kumar[61] was tabulated in Table 7. Kumar[80] conducted the axial impact load on Al cylindrical tube for comparison with three different Al/composite cylindrical tubes to investigate their impact performance for meeting the needs of crashworthiness characteristics. The initial peak force (IPF) of the Al cylindrical tube was higher than Al/composite cylindrical tubes but the result of the specific energy absorption (SEA) of the Al cylindrical tube was opposite to IPF.

Table 7. Comparison of perforation energy between metal and FMLs.

References	Perforation energy (J)		
[60]	Al 2024-T3 alloy	GLARE 5-2/1	GLARE 4-3/2
	33.4	34.5	38.5
[66]	Al 2024-T3 alloy	Woven-based GLARE	UD-based GLARE
	15	55	55
[61]	Al 6061 alloy	Woven-based GEAML	CSM-based GEAML
	6.321	6.357	6.148

Zhu et al.[46] conducted an axial quasi-static crushing test at a loading rate of 4mm/min to examine the crushing behavior of Al tubes (AL-in and AL-out). The external diameters of AL-in and AL-out were 57.10mm and 63.79mm, respectively, while their thickness, length, and density were equal. Results indicated that the Al tubes underwent the elastic stage and progressive folding stage. AL-out obtained the highest initial peak load (39.7kN) during the elastic stage compared to AL-in (36.4kN). Several oscillations appeared in the force-displacement curves as the Al tubes deformed plastically during the stage of progressive folding. The progressive folding stage was the primary energy absorption phase. The AL-out had better energy absorption, peak crushing force, and mean crushing force than AL-in. The thickness of Al-out may influence its impact performance[46]. The results obtained were similar to Fie et al.[81] who conducted the Al tube with different diameters in the axial crushing test[81].

Karagiozova and Jones[82,83] reported that the development of the buckling shape of a square tube was influenced by the impact velocity and mass of a striker when considering the transient deformation process. The transient deformation process in elastic–plastic square tubes subjected to axial impact loads demonstrated that the beginning of buckling was greatly impacted by propagating elastic and plastic stress waves. Plastic waves generated by an axial impact propagated faster in square tubes than in circular tubes. When subjected to impact velocities between 14.84 and 98.27 m/s, the square tubes tested here exhibited either dynamic progressive or dynamic plastic buckling, meanwhile the corresponding circular tubes exhibited only dynamic progressive buckling. Karagiozova and Alves[84] also reported that the transition conditions between two collapse modes (progressive buckling and global bending) of Al alloy circular tubes, were significantly influenced by the axial impact velocity. The tube was more stable as impact velocity increased. For example, progressive buckling can occur for long tubes. However, the longer tube can cause the beginning of the desired buckling mode more complex and exhibited multiple buckling modes, resulting in insufficient energy absorption[85]. Besides that, due to the change in bending rigidity caused by material hardening and yield stress of the material models, the material characteristics also influenced the buckle pattern. It has been shown that circular tubes constructed of ductile alloys with high yield stress and low strain hardening characteristics performed better as energy absorbers than circular tubes constructed of alloys with low yield stress and high strain hardening characteristics[84]. Moreover, Jensen et al.[86] reported that the buckling transition varied depending not only on the impact velocity but also on the width-to-thickness ratio.

In conclusion, an impact test on metal was conducted for comparison with FML and composite laminate. In another word, it served as baseline material. For example, the Al sheet had the worst impact characteristics such as lower specific perforation energy and energy absorption compared to FML and composite laminate[60,61,66,87]. However, the Al sheet had a longer crack initiation life than FML[35]. The greater diameter of the Al tube exhibited better energy absorption and peak crushing force. It can be concluded that the thickness of the Al tube influenced the impact performance[46, 81]. On the other hand, the transition condition or buckling shape of the alloy tube subjected to axial impact loading was influenced by impact velocity[82–84], striking mass[82,83], material characteristic[84] and the width-to-thickness ratio[86].

3. Axial impact test on FMLs

The objective of the axial impact test on FML is to determine the impact properties of FML under axial loading or in-plane direction. However, there was insufficient and limited research that examined this type of impact loading. According to previous literature, strain rate, lay-up sequence of composite, strain rate, geometry and other factors have been found to influence the crushing behavior of hybrid components.

El-Hage et al.[87] used a computational method to examine the effects of the number of layers, fibre orientation and inner metallic wall thickness on the axial crushing behaviors of metal/composite hybrid tubes. They found that thinner Al tubes could make the crush resistance better and that the hybrid tubes could absorb the most energy when the angle of the composite fibres was 90°. Bambach et al.[88] conducted extensive experimental testing to examine the crushing behaviors of steel square hollow sections reinforced with CFRP. They found that using CFRP could enhance the axial loading capacity by limiting the growth of elastic buckling deflections and delaying local buckling. Kim et al.[89] examined how fibre orientation and lay-up sequence affected failure mechanisms and crash characteristics of an Al/CFRP hybrid column under dynamic axial loading.

Ahmad et al.[90] studied the crush response and energy absorption capacity of FML thin-walled tubes and compared them with Al and composite tubes. Results indicated that FML tubes were favored as impact energy absorbers because they could sustain greater impact loads,

therefore absorbing more energy. FML tubes had better loading capacity as the crush length increased. The presence of metallic and composite layer stacks appeared to enhance the crush resistance and capacity to absorb the energy of the tubular structure[89,91,92]. It can be concluded that the energy absorption capacity increased as deflection and the number of tube layers increased. Eyvazian et al.[93] investigated the crushing behavior of corrugated metal-composites tubes subjected to axial loading. The addition of composite layers to the corrugated metal tube improved the metal tube's energy absorption capability. The composite layers made the tube more resistant to elastic deformation as the initial peak load of the corrugated metal-composite tube was greater than a corrugated metal tube. The corrugated metal-composite tube exhibited minimal fluctuation in the force-displacement curve and underwent consistent crushing mode. Hence, the specific energy absorption of corrugated metal-composite was 53% higher than the corrugated metal tube.

Subbaramaiah et al.[94] compared the behavior of the GLARE 2/1 top-hat structure to the Al structure under axial crushing. The crushing strength and SEA of the GLARE top-hat structure were excellent compared to the Al structure, as shown in Fig. 9.

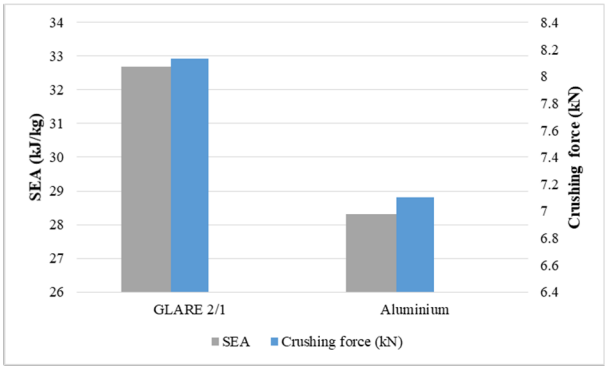

Fig. 9. Crushing force and SEA of GLARE 2/1 and Al top-hat structure[94].

The failure modes that occurred during the axial crushing of the FML were a combination of GFRP and Al failure mechanisms. The Al layer experienced plastic deformations such as folding and tearing. Failure modes of composite layers include splaying, delamination, cracking, matrix debris, fibre and laminar failure. Fig. 10 showed the crushing failure modes in the FML structure. The researchers discovered that GLARE was superior to the Al alloy in terms of crushing strength and energy absorption capacity by 9% and 16%, respectively.

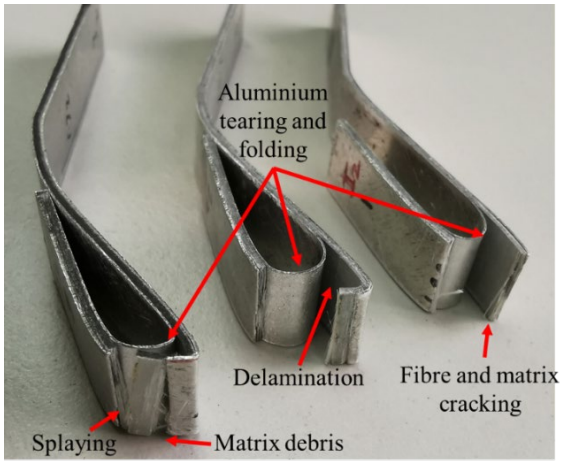

Fig. 10: FML crushing failure modes.

Subbaramaiah et al.[95] found that when a composite was bonded to a metal substrate, the energy absorption and crushing strength were both higher than when the metal substrate was used alone. Shin et al.[41] investigated the energy-absorbing capability of axial crushing of square Al/GFRP hybrid tubes (0˚, 90˚, 0˚/90˚ and ±45˚ fibre orientations). The square Al/GFRP hybrid tube with fibre in the 90˚ direction demonstrated greater energy absorption capability in comparison to others. The tube was crushed with a stable local buckling failure mechanism because the composite laminate prevented the Al tube from folding. A comparable study was conducted by Song et al.[96] on circular tubes. However, Kim et al.[89] discovered that the Al/CFRP hybrid square hollow section (SHS) beam with fibre in the 0˚/90˚ direction exhibited the highest energy absorption. When the thickness of CFRP laminate increased, its crashworthiness performance was enhanced in terms of SEA and CFE.

Ge et al.[81] compared the EA, SEA, PCF and CFE between Al/CFRP (1/1) and Al/CFRP/Al (2/1) hybrid tubes under axial crushing. Table 8 indicates that the impacts of geometry size and fibre lay-up sequence on the axial crushing energy-absorption performances of the two hybrid tube types were compared. Results indicated that the energy absorption of the specimens with [0˚/90˚] lay-up sequence was greater than that of the specimens with [45˚/−45˚] lay-up sequence for both types of hybrid tubes. To produce a stable and controllable progressive crushing failure mode, the author recommended that the appropriate length of the tubes should be chosen to avoid a length-to-diameter ratio that is too tiny. The geometric size had little effect on the specific energy absorption and crushing force efficiency of the 2/1 hybrid tubes.

Table 8. Comparison of energy-absorption performance between 1/1 and 2/1 hybrid tubes[81].

		EA (kJ)		SEA (J/g)		PCF (kN)		CFE	
		L=105mm D=38mm	L=132 D=38mm	L=105mm D=38mm	L=132 D=38mm	L=105mm D=38mm	L=132 D=38mm	L=105mm D=38mm	L=132 D=38mm
1/1	45°/-45°	1.83	2.27	43.18	47.00	51.62	52.14	0.51	0.54
	0°/90°	2.77	2.70	65.07	55.95	78.11	74.04	0.51	0.46
		L=105mm D=44mm	L=132 D=44mm	L=105mm D=44mm	L=132 D=44mm	L=105mm D=44mm	L=132 D=44mm	L=105mm D=44mm	L=132 D=44mm
2/1	45°/-45°	4.17	4.79	45.52	45.57	141.7	135.7	0.42	0.44
	0°/90°	4.26	5.65	46.57	53.67	170.1	156.0	0.36	0.45

Zhu et al.[46] conducted an axial quasi-static crushing test at a loading rate of 4mm/min to examine the crushing behavior of hybrid tubes: H-I (AL-out tube internally filled with the CFRP tube), H-II (CFRP tube internally filled with the AL-in), and H-III (inner AL-in tube and outer AL-out tube sandwiched with a CFRP tube core) and compared them to carbon fibre-reinforced polymer (CFRP) and Al tubes. The results indicated that the optimal configuration was the H-I hybrid tube compared to H-II and H-III hybrid tubes. Because of the complex continuous interaction and the change in deformation modes, the hybrid tube H-I absorbed roughly 30% more energy than the energy absorbed by the CFRP tube and AL-out tube. The hybrid tube H-II had 11% less energy absorption than the total energy absorption of CFRP and Al tubes. This was because the Al tube caused the CFRP tube's failure mode to change from mode I (longitudinal crack) to mode II (CFRP tube bent and deformed). Subsequently, it broke into some big fragments and eventually lost its load-bearing capability. Overall, H-III tubes absorbed more energy than CFRP and Al tubes. The SEA of hybrid tube H-III was however less than that of hybrid tube H-I and hybrid tube H-II, indicating that hybrid tube H-III was the least efficient in terms of energy absorption.

Zhang et al.[97] conducted the axial impact test on carbon-fibre/epoxy laminated composite slender beams with different layup configurations $([0_{12}], [(\pm 22.5^{\circ})_3]_s, [(\pm 45^{\circ})_3]_s, [(\pm 67.5)_3]_s, [(0^{\circ}/90^{\circ})_3]_s, [(0^{\circ}/90^{\circ})_2/0^{\circ}_2]_s)$. It is reviewed here because it is the closest to FML under axial impact and could give significant fundamental understanding. The purpose of this paper was to examine the initiation and mechanisms of damage on the impacted composite by a moving mass. They emphasized that the slender structural components were susceptible to buckling under static or dynamic loads[97]. Matrix cracking and delamination were found to be the most prominent defects within the beams except for the beams with $[0_{12}]$ and $[(\pm 67.5)_3]$s layups. The majority of beams with $[(\pm 67.5)_3]$s layup, exhibited neither delamination nor matrix crack, but the deformed shape was maintained due to the matrix's plastic deformation. For beams with $[0_{12}]$ layup, matrix cracking occurred perpendicular to the fibre direction and the beam fractured into two or more pieces. Initial voids caused by manufacturing are not negligible. Delamination occurred at the inter-laminar interfaces and its propagation was dependent on the energy absorbed by the beam and the layup sequences. The layup sequences and slenderness ratio had a substantial effect on the critical energy for initiating damage[98]. The slenderness ratio is the ratio of length (l) to the radius of gyration (k), l/k. This paper significantly focused on the energy required to initiate damage and was similar to my research in investigating the impact response of FML with different layup sequences under axial impact.

In conclusion, the research on the experimental axial impact test of FML structure was very limited. The most tested FML structures were in form of tubes (circular/cylindrical, square). The influence of FML's constituents (composite and metal alloy), fibre orientation, stacking sequence, metal arrangement and laminate thickness played a role in determining the crushing behavior and improving the crush stability and energy absorption of FML structures[41, 46, 81, 87–92, 95]. The FML structure had better crushing strength compared to the metal structure[94–96]. Buckling, delamination, matrix cracking, fibre failure and plastic deformation were the failure modes and failure mechanisms that occurred in FML structure[97, 98]. However, additional research is required to analyze and get a deeper understanding of the experimental axial impact test of FML and its components.

Conclusion

Literature showed FMLs have a significant amount of potential in a variety of applications, such as aircraft, automotive, marine, sporting goods, medicine, and miscellaneous. In many circumstances, the mechanical properties of FMLs are better than those of traditional metal alloys or fibre-reinforced polymer composites. Major benefits of FMLs include excellent fatigue properties, a high modulus of elasticity with increased toughness, and a high strength-to-weight ratio. This paper reviewed the history of FML, the classification of FML, its applications and mechanical properties, and the response or performance of FMLs to impact loading based

on experimental work. Response of FML to impact loading is dependent on several variables, including impact energy (varying the impact velocity or drop height), fibre orientation, direction and type of reinforcement, layup configuration, stacking sequence, metal arrangement, number of impacts, indenter size, geometry (thickness of metal/laminate, width, and length), and material properties. Energy absorption (EA), specific energy absorption (SEA), mean crushing force (Fmean), peak crushing force (PCF) or peak load (Pmax) and crush force efficiency (CFE) are some of the indicators that can be used to measure the impact performance of FML. Overall, the literature on the response of FML flat plate structures to axial impact loads is unreported, and the most current research focusing on the axial crushing of FML tubes. Hence, further studies are required to increase the applicability of FMLs in applications that may be impacted under axial loading.

Acknowledgements

This project is funded by the Ministry of Higher Education (MOHE) of Malaysia, ref no. FRGS/1/2018/TK03/UiTM/02/5. Thank you to Universiti Teknologi MARA, Malaysia for various and generous assistance throughout the project until completion.

Nomenclature

Al	aluminium
ARALL	aramid-reinforced aluminium laminate
CAJRALL	carbon-jute reinforced aluminium laminate
CAJRMAL	carbon-jute reinforced magnesium laminate
CARALL	carbon-reinforced aluminium laminate
CFE	crushing force efficiency
CFRP	carbon fibre-reinforced polymer
CSM	chopped strand mat
EA	energy absorption
FML	fibre metal laminate
FRP	fibre-reinforced polymer
GFPP	glass fibre-reinforced polypropylene
GFRP	glass fibre-reinforced polymer
GLARE	glass reinforced aluminium laminate
HTCL	hybrid titanium-carbon composite laminates
HVI	high velocity impact
IPF	initial peak force
LVI	low velocity impact
MVF	metal volume fraction
N/A	not available
PCF	peak crushing force
ROM	rules of mixture
SEA	specific energy absorption
SHS	square hollow section
UD	unidirectional
l	length
k	radius of gyration

References

1) Z. Ding, H. Wang, J. Luo, and N. Li, "A review on forming technologies of fibre metal laminates," *Int. J. Light. Mater. Manuf.*, **4** (*1*) 110–126 (2021). doi:10.1016/j.ijlmm.2020.06.006.
2) A. Kumar, A.K. Chanda, and S. Angra, "Numerical modelling of a composite sandwich structure having non metallic honeycomb core," *Evergreen*, **8** (*4*) 759–767 (2021). doi:10.5109/4742119.
3) M. Maurya, N.K. Maurya, and V. Bajpai, "Effect of sic reinforced particle parameters in the development of aluminium based metal matrix composite," *Evergreen*, **6** (*3*) 200–206 (2019). doi:10.5109/2349295.
4) S. Kabir, F. Ahmad, K. Malik, N. Nosbi, and L. Gui Llaumat, "Effect of heat resistant coating on the drilled hole quality of hybrid fiber reinforced epoxy composite," *Evergreen*, **7** (*4*) 530–537 (2020). doi:10.5109/4150472.
5) R. Yadav, S.P. Dwivedi, and V.K. Dwivedi, "Effect of casting parameters on tensile strength of chrome containing leather waste reinforced aluminium based composite using rsm," *Evergr. Jt. J. Nov. Carbon Resour. Sci. Green Asia Strateg.*, **09** (*04*) 1031–1038 (2022).
6) E.C. Botelho, R.A. Silva, L.C. Pardini, and M.C. Rezende, "A review on the development and properties of continuous fiber/epoxy/aluminum hybrid composites for aircraft structures," *Mater. Res.*, **9** (*3*) 247–256 (2006). doi:10.1590/S1516-14392006000300002.
7) M.E. Novianta, A.E. Ismail, and K.A. Kamarudin, "Roles of layers and fiber orientations on the mechanical durability of hybrid composites," *Model. Damage Process. Biocomposites, Fibre-Reinforced Compos. Hybrid Compos.*, 41–56 (2018). doi:10.1016/B978- 0-08-102289-4.00004-7.
8) D.K. Rajak, D.D. Pagar, P.L. Menezes, and E. Linul, "Fiber-reinforced polymer composites : manufacturing, properties, and applications," *Polymers (Basel).*, **11** (*1667*) (2019).
9) D. Choudhari, and V. Kakhandki, "Characterization and analysis of mechanical properties of short carbon fiber reinforced polyamide66 composites," *Evergreen*, **8** (*4*) 768–776 (2021). doi:10.5109/4742120.
10) A. Kumar, A.K. Chanda, and S. Angra, "Optimization of stiffness properties of composite sandwich using

hybrid taguchi-gra-pca," *Evergreen*, **8** (*2*) 310–317 (2021). doi:10.5109/4480708.

11) R. Alderiesten, "Fatigue in fibre metal laminates: the interplay between fatigue in metals and fatigue in composites," *Fatigue Fract. Eng. Mater. Struct.*, **42** (*11*) 2414–2421 (2019). doi:10.1111/ffe.12995.
12) J. Bieniaś, P. Jakubczak, and B. Surowska, "Properties and characterization of fiber metal laminates," *Hybrid Polym. Compos. Mater. Prop. Characterisation*, 253–277 (2017). doi:10.1016/B978-0-08-100787-7.00011-1.
13) E. Hariharan, and R. Santhanakrishnan, "Experimental analysis of fiber metal laminate with aluminium alloy for aircraft structures," *Int. J. Eng. Sci. Res. Technol.*, **9655** (*5*) 94–102 (2016).
14) A. Salve, R. Kulkarni, and A. Mache, "A review : fiber metal laminates (fml's) - manufacturing, test methods and numerical modeling," *Int. J. Eng. Technol. Sci.*, **6** (*1*) 71–84 (2016). doi:http://dx.doi.org/10.15282/ijets.6.2016.10.2.1060 A.
15) M. Kashfi, G.H. Majzoobi, N. Bonora, G. Iannitti, A. Ruggiero, and E. Khademi, "A study on fiber metal laminates by using a new damage model for composite layer," *Int. J. Mech. Sci.*, **131**–**132** (*June*) 75–80 (2017). doi:10.1016/j.ijmecsci.2017.06.045.
16) M. Vasumathi, and V. Murali, "Effect of alternate metals for use in natural fibre reinforced fibre metal laminates under bending , impact and axial loadings," in: Int. Conf. Des. Manuf. IConDM 2013, Elsevier B.V., 2013: pp. 562–570. doi:10.1016/j.proeng.2013.09.131.
17) A. Harichandan, and K.R. Vijaya Kumar, "Study on tensile behaviour of carbon jute aluminium- fibre metal laminates," *Int. J. Mech. Prod. Eng.*, **4** (*7*) 38–42 (2016).
18) J. Jerome, N. Rajesh Jesudoss Hynes, and R. Sankaranarayanan, "Mechanical behavioural testing of fibre metal laminate composites," *AIP Conf. Proc.*, **2220** (*May*) (2020). doi:10.1063/5.0001244.
19) J. Sinke, "Manufacturing principles for fiber metal laminates," in: ICCM Int. Conf. Compos. Mater., 2009.
20) H. Abramovich, "Introduction to composite materials," *Stab. Vib. Thin-Walled Compos. Struct.*, 1–47 (2017). doi:10.1016/B978-0-08-100410-4.00001-6.
21) M. Kamocka, and R.J. Mania, "Analytical and experimental determination of fml stiffness and strength properties," *Mech. Mech. Eng.*, **19** (*2*) 141–159 (2015).
22) A. Asundi, and A.Y.N. Choi, "Fiber metal laminates: an advanced material for future aircraft," *J. Mater. Process. Technol.*, **63** (*1–3*) 384–394 (1997). doi:10.1016/S0924-0136(96)02652-0.
23) R. Das, A. Chanda, J. Brechou, and A. Banerjee, "17 – impact behaviour of fibre–metal laminates," *Dyn. Deform. Damage Fract. Compos. Mater. Struct.*, 491–542 (2016). doi:10.1016/B978-0-08-100080-9.00017-8.
24) A.M. Mukesh, and N. Rajesh Jesudoss Hynes, "Mechanical properties and applications of fibre metal laminates," in: AIP Conf. Proc. 2142, 100002, AIP Publishing, 2019. doi:10.1063/1.5122456.
25) A. Islam, S.P. Dwivedi, V.K. Dwivedi, and R. Yadav, "Extraction of chromium oxide from cclw to develop the aluminium based composite by fsp as reinforcement alongwith alumina," *Evergreen*, **09** (*04*) 993–1002 (2022).
26) C.P. Zhen, "Review on the dynamic impact characteristics of fiber metal laminates," *J. Adv. Rev. Sci. Res.*, **16** (*1*) 1–11 (2015).
27) S. Krishnakumar, "Fiber Metal Laminates — The Synthesis of Metals and Composites," 1994. doi:10.1080/10426919408934905.
28) S.Y. Park, and W.J. Choi, "The Guidelines of Material Design and Process Control on Hybrid Fiber Metal Metal Laminate for Aircraft Structures," in: K. Maalawi (Ed.), Optim. Compos. Struct., IntechOpen, 2018: p. 204. doi:10.5772/intechopen.78217.
29) E. Sherkatghanad, L. Lang, H. Blala, L. Li, and S. Alexandrov, "Fiber metal laminate structure, a good replacement for monolithic and composite materials," *IOP Conf. Ser. Mater. Sci. Eng.*, **576** (*1*) (2019). doi:10.1088/1757-899X/576/1/012034.
30) S.Y. Park, W.J. Choi, H.S. Choi, and H. Kwon, "Effects of surface pre-treatment and void content on glare laminate process characteristics," *J. Mater. Process. Technol.*, **210** (*8*) 1008–1016 (2010). doi:10.1016/j.jmatprotec.2010.01.017.
31) S. Zhu, and G.B. Chai, "Low-velocity impact response of fibre-metal laminates-experimental and finite element analysis," *Compos. Sci. Technol.*, **72** (*15*) 1793–1802 (2012). doi:10.1016/j.compscitech.2012.07.016.
32) S.D. Malingam, K.A. Zakaria, N.M. Ishak, and M.R. Mansor, "Application of triz to develop natural fibre metal laminate for car front hood," *ARPN J. Eng. Appl. Sci.*, **13** (*1*) (2018).
33) S.D. Malingam, K. Subramaniam, F.A. Jumaat, A.F.A. Ghani, and L.F. Ng, "Tensile and impact properties of cost- - effective hybrid fiber metal laminate sandwich structures," *WILEY*, (*October 2017*) 2385–2393 (2018). doi:10.1002/adv.21913.
34) J.-M. Yang, T.H. Hahn, H. Seo, P.-Y. Chang, and P.-C. Yeh, "Damage Tolerance and Durability of Fiber-Metal Laminates for Aircraft Structures," U.S. Department of Transportation Federal Aviation Administration Air Traffic Organization NextGen & Operations Planning Office of Research and Technology Development Washington, DC 20591, 2010.
35) H. Seo, H.T. Hahn, and J. Yang, "Impact damage tolerance and fatigue durability of glare laminates," *Eng. Mater. Technol.*, **130** (*October 2008*) 1–6 (2015).

doi:10.1115/1.2969253.
36) B. Surowska, P. Jakubczak, and C. Outline, "Impact resistance and damage of fiber metal laminates," Lublin University of Technology, Lublin, Poland, 2017. doi:10.1016/B978-0-08-100787-7.00012-3.
37) I. Mohammed, A.R.A. Talib, M. Thariq, M.T.H. Sultan, and S. Saadon, "Fire behavioural and mechanical properties of carbon fibre reinforced aluminium laminate composites for aero-engine," *Int. J. Eng. Technol.*, **7** 22–27 (2018).
38) M. Hozumi, A. Jumahat, N. Sapiai, and Z. Salleh, "Effect of fibre architecture on impact response of glass-aluminium fibres metal laminates (fml)," *Int. J. Eng. Adv. Technol.*, **9** (*1*) 5639–5645 (2019). doi:10.35940/ijeat.A3039.109119.
39) B. Rakham, and D. Giridharan, "Experimental analysis of fibre metal laminates," *IOP Conf. Ser. Mater. Sci. Eng.*, **455** (*012037*) (2018). doi:10.1088/1757-899X/455/1/012037.
40) J.F. Laliberté, C. Poon, P. V. Straznicky, and A. Fahr, "Application of fiber-metal laminates," *Polym. Compos.*, **21** (*4*) 558–567 (2000). source: http://onlinelibrary.wiley.com/doi/10.1002/pc.10211/full/#.WWw4CZaE-aA.mendeley%0A%0A.
41) K.C. Shin, J.J. Lee, K.H. Kim, M.C. Song, and J.S. Huh, "Axial crush and bending collapse of an aluminum/gfrp hybrid square tube and its energy absorption capability," *Compos. Struct.*, **57** (*1–4*) 279–287 (2002). doi:10.1016/S0263-8223(02)00094-6.
42) N.M. Ishak, S.D. Malingam, M.R. Mansor, N. Razali, Z. Mustafa, and A.F.A. Ghani, "Investigation of natural fibre metal laminate as car front hood," *Mater. Res. Express*, **8** (*2*) (2021). doi:10.1088/2053-1591/abe49d.
43) V.N.P.M. Pariti, "Mechanical behavior of carbon and glass fiber reinforced composite materials under varying loading rates," 2017.
44) M.S. Yaakob, M.N. Abdullah, M.K.H. Muda, and F. Mustapha, "Drop-weight impact test for measuring the damage resistance of aero helmets," *J. Adv. Res. Appl. Mech.*, **8** (*1*) 31–39 (2015).
45) A.S. Abdullah, "Crash simulation of fibre metal laminate fuselage," University of Manchester, 2014.
46) G. Zhu, G. Sun, Q. Liu, G. Li, and Q. Li, "On crushing characteristics of different configurations of metal-composites hybrid tubes," *Compos. Struct.*, **175** 58–69 (2017). doi:10.1016/j.compstruct.2017.04.072.
47) T. Trzepiecinski, A. Kubit, R. Kudelski, P. Kwolek, and A. Obłój, "Strength properties of aluminium/glass-fiber-reinforced laminate with additional epoxy adhesive film interlayer," *Int. J. Adhes. Adhes.*, **85** 29–36 (2018). doi:10.1016/j.ijadhadh.2018.05.016.
48) P. Jakubczak, J. Bienia, M. Drozdziel, P. Podolak, and A. Harmasz, "The effect of layer thicknesses in hybrid titanium-carbon laminates on low-velocity impact response," *Materials (Basel).*, **13** (*103*) 1–17 (2020).
49) R Lokesh, V Jagadesh, and S Suresh, "Mechanical and low velocity impact behavior of al based kevlar fabric reinforced epoxy laminate," *Int. J. Appl. Eng. Res.*, **16** (*8*) 660–669 (2021).
50) A.S. Yaghoubi, Y. Liu, and B. Liaw, "Low-velocity impact on glare 5 fiber-metal laminates: influences of specimen thickness and impactor mass," *J. Aerosp. Eng.*, (*July*) 409–420 (2012). doi:10.1061/(ASCE)AS.1943-5525.0000134.
51) P. Sathyaseelan, K. Logesh, M. Venkatasudhahar, and N.D. Raja, "Experimental and finite element analysis of fibre metal laminates (fml's) subjected to tensile, flexural and impact loadings with different stacking sequence," *Int. J. Mech. Mechatronics Eng. IJMME-IJENS*, **15** (*03*) 23–27 (2015).
52) A.P. Sharma, S.H. Khan, R. Kitey, and V. Parameswaran, "Effect of through thickness metal layer distribution on the low velocity impact response of fiber metal laminates," *Polym. Test.*, **65** (*December 2017*) 301–312 (2018). doi:10.1016/j.polymertesting.2017.12.001.
53) S.H. Khan, A.P. Sharma, R. Kitey, and V. Parameswaran, "Effect of metal layer placement on the damage and energy absorption mechanisms in aluminium/glass fibre laminates," *Int. J. Impact Eng.*, **119** (*November 2017*) 14–25 (2018). doi:10.1016/j.ijimpeng.2018.04.011.
54) N. Tsartsaris, M. Meo, F. Dolce, U. Polimeno, M. Guida, and F. Marulo, "Low-velocity impact behaviour of fibre metal laminates," *Compos. Mater.*, **45** (*7*) 803–814 (2011). doi:10.1177/0021998310376108.
55) A.A. Ramadhan, A.R. Abu Talib, A.S. Mohd Rafie, and R. Zahari, "The behaviour of fibre-metal laminates under high velocity impact loading with different stacking sequences of al alloy," *Appl. Mech. Mater.*, **225** 213–218 (2012). doi:10.4028/www.scientific.net/AMM.225.213.
56) F.D. Morinière, R.C. Alderliesten, M. Sadighi, and R. Benedictus, "An integrated study on the low-velocity impact response of the glare fibre-metal laminate," *Compos. Struct.*, **100** 89–103 (2013). doi:10.1016/j.compstruct.2012.12.016.
57) M. Sadighi, R.C. Alderliesten, M. Sayeaftabi, and R. Benedictus, "Experimental and numerical investigation of metal type and thickness effects on the impact resistance of fiber metal laminates," *Appl. Compos. Mater.*, **19** 545–559 (2012). doi:10.1007/s10443-011-9235-6.
58) R. Starikov, "Assessment of impact response of fiber metal laminates," *Int. J. Impact Eng.*, **59** 38–45 (2013). doi:10.1016/j.ijimpeng.2013.02.008.
59) J. Fan, W. Cantwell, and Z. Guan, "The low-velocity impact response of fiber-metal laminates," *Reinf.*

Plast. Compos., **30** (*1*) 26–35 (2011). doi:10.1177/0731684410386133.

60) G. Wu, J.-M. Yang, and H.T. Hahn, "The impact properties and damage tolerance and of bi-directionally reinforced fiber metal laminates," *Mater. Sci.*, **42** 948–957 (2007). doi:10.1007/s10853-006-0014-y.
61) V. Asha Melba, and A. Senthil Kumar, "Impact response and damage resistance behavior of gfrp/aluminium fiber metal laminates during low velocity impact test," *Indian J. Eng. Mater. Sci.*, **25** (*6*) 450–458 (2018).
62) M. Kutz, "Handbook of materials evaluation," 1988. doi:10.1016/0142-9612(88)90055-5.
63) N.K. Romli, M.R.M. Rejab, D. Bachtiar, J. Siregar, M.F. Rani, W.S.W. Harun, S.M. Salleh, and M.N.M. Merzuki, "The behavior of aluminium carbon/epoxy fibre metal laminate under quasi-static loading," *IOP Conf. Ser. Mater. Sci. Eng.*, **257** (*1*) (2017). doi:10.1088/1757-899X/257/1/012046.
64) A.S. Yaghoubi, and B. Liaw, "Experimental and numerical approaches on behavior of glare 5 beams : influences of thickness and stacking sequence," *Conf. Proc. Soc. Exp. Mech. Ser. 31*, **6** 7–16 (2012). doi:10.1007/978-1-4614-2419-2.
65) F. Taheri-Behrooz, M.M. Shokrieh, and I. Yahyapour, "Effect of stacking sequence on failure mode of fiber metal laminates under low-velocity impact," *Iran. Polym. J.*, **23** (*2*) 147–152 (2014). doi:10.1007/s13726-013-0210-y.
66) G.R. Villanueva, and W.J. Cantwell, "The high velocity impact response of composite and fml-reinforced sandwich structures," *Compos. Sci. Technol.*, **64** 35–54 (2004). doi:10.1016/S0266-3538(03)00197-0.
67) G.S.E. Bikakis, A. Savaidis, P. Zalimidis, and S. Tsitos, "Influence of the Metal Volume Fraction on the permanent dent depth and energy absorption of GLARE plates subjected to low velocity impact," in: 20th Innov. Manuf. Eng. Energy Conf., 2016: pp. 1–9. doi:10.1088/1757-899X/161/1/012055.
68) G.S.E. Bikakis, A. Savaidis, P. Zalimidis, and S. Tsitos, "Influence of the Metal Volume Fraction on the maximum deflection and impact load of GLARE plates subjected to low velocity impact," in: 20th Innov. Manuf. Eng. Energy Conf., 2016: pp. 1–10. doi:10.1088/1757-899X/161/1/012054.
69) E. Guades, T. Aravinthan, A. Manalo, and M. Islam, "Experimental investigation on the behaviour of square frp composite tubes under repeated axial impact," *Compos. Struct.*, **97** 211–221 (2013). doi:10.1016/j.compstruct.2012.10.033.
70) N. Shaari, A. Jumahat, and M.K.M. Razif, "Impact resistance properties of kevlar/glass fiber hybrid composite laminates," *J. Teknol.*, **76** (*3*) 93–99 (2015). doi:10.11113/jt.v76.5520.
71) S. Ray, "Effect of control parameters on erosion wear performance of glass-epoxy composites filled with waste marble powder," *Evergreen*, **9** (*1*) 23–31 (2022). doi:10.5109/4774213.
72) A. Mahyudin, S. Arief, H. Abral, Emriadi, M. Muldarisnur, and M.P. Artika, "Mechanical properties and biodegradability of areca nut fiber-reinforced polymer blend composites," *Evergreen*, **7** (*3*) 366–372 (2020). doi:10.5109/4068618.
73) H. Sosiati, Y.A. Shofie, and A.W. Nugroho, "Tensile properties of kenaf/e-glass reinforced hybrid polypropylene (pp) composites with different fiber loading," *Evergreen*, **5** (*2*) 1–5 (2018). doi:10.5109/1936210.
74) H. Sosiati, N.D.M. Yuniar, D. Saputra, and S. Hamdan, "The influence of carbon fiber content on the tensile, flexural, and thermal properties of the sisal/pmma composites," *Evergreen*, **9** (*1*) 32–40 (2022). doi:10.5109/4774214.
75) W.H. Choong, K.B. Yeo, and M.T. Fadzlita, "Impact damage behaviour of woven glass fibre reinforced polymer composite," *J. Appl. Sci.*, **11** (*13*) 2440–2443 (2011).
76) C. Evci, and M. Gülgeç, "An experimental investigation on the impact response of composite materials," *Int. J. Impact Eng.*, **43** 40–51 (2012). doi:10.1016/j.ijimpeng.2011.11.009.
77) V. K. Srivastava, "Impact behaviour of sandwich gfrp-foam-gfrp composites," *Int. J. Compos. Mater.*, **2** (*4*) 63–66 (2012). doi:10.5923/j.cmaterials.20120204.04.
78) P.H. Bull, and F. Edgren, "Compressive strength after impact of cfrp-foam core sandwich panels in marine applications," *Compos. Part B Eng.*, **35** (*6–8*) 535–541 (2004). doi:10.1016/j.compositesb.2003.11.007.
79) G. Zhu, G. Werner, and C.K.H. Dharan, "Penetration of laminated kevlar by projectiles-l. experimental investigation," *Solid Struct.*, **29** (*1975*) 399–420 (1991).
80) A.P. Kumar, "Experimental analysis on the axial crushing and energy absorption characteristics of novel hybrid aluminium/composite-capped cylindrical tubular structures," *Proc. Inst. Mech. Eng. Part L J. Mater. Des. Appl.*, **233** (*11*) 2234–2252 (2019). doi:10.1177/1464420719843157.
81) F. Ge, Y. Lin, F. Zhang, Z. Zhang, and M. Wang, "Crushing characteristics comparison between aluminum/cfrp and aluminum/cfrp/aluminum hybrid tubes," *Polymers (Basel).*, **14** (*19*) (2022). doi:10.3390/polym14194034.
82) D. Karagiozova, and N. Jones, "Dynamic buckling of elastic-plastic square tubes under axial impact-ii : structural response," *Int. J. Impact Eng.*, **30** 167–192 (2004). doi:10.1016/S0734-743X(03)00062-9.
83) D. Karagiozova, and N. Jones, "Inertia effects in square tubes subjected to an axial impact," *Struct. Under Shock Impact VII*, 1–10 (2002).
84) D. Karagiozova, and M. Alves, "Transition from

progressive buckling to global bending of circular shells under axial impact-part i: experimental and numerical observations," *Int. J. Solids Struct.*, **41** 1565–1580 (2004). doi:10.1016/j.ijsolstr.2003.10.005.

85) W. Abramowicz, and N. Jones, "Transition from initial global bending to progressive buckling of tubes loaded statically and dynamically," *Int. J. Impact Enginerring*, **19** (*96*) (1997).
86) O. Jensen, M. Langseth, and O.S. Hopperstad, "Transition between progressive and global buckling of aluminium extrusions," *Struct. Under Shock Impact VII*, (2002).
87) H. El-Hage, P.K. Mallick, and N. Zamani, "A numerical study on the quasi-static axial crush characteristics of square aluminum-composite hybrid tubes," *Compos. Struct.*, **73** (*4*) 505–514 (2006). doi:10.1016/j.compstruct.2005.03.004.
88) M.R. Bambach, H.H. Jama, and M. Elchalakani, "Axial capacity and design of thin-walled steel shs strengthened with cfrp," *Thin-Walled Struct.*, **47** (*10*) 1112–1121 (2009). doi:10.1016/j.tws.2008.10.006.
89) H.C. Kim, D.K. Shin, J.J. Lee, and J.B. Kwon, "Crashworthiness of aluminum/cfrp square hollow section beam under axial impact loading for crash box application," *Compos. Struct.*, **112** (*1*) 1–10 (2014). doi:10.1016/j.compstruct.2014.01.042.
90) Z. Ahmad, M.R. Abdullah, and M.N. Tamin, "Experimental and numerical studies of fiber metal laminate (fml) thin-walled tubes under impact loading," *Adv. Struct. Mater.*, **70** 433–443 (2015). doi:10.1007/978-3-319-19443-1_35.
91) J.S. Lin, X. Wang, and G. Lu, "Crushing characteristics of fiber reinforced conical tubes with foam-filler," *Compos. Struct.*, (2014). doi:http://dx.doi.org/10.1016/j.compstruct.2014.04.023.
92) F. Tarlochan, F. Samer, A.M.S. Hamouda, S. Ramesh, and K. Khalid, "Design of thin wall structures for energy absorption applications: enhancement of crashworthiness due to axial and oblique impact forces," *Thin-Walled Struct.*, **71** 7–17 (2013). doi:10.1016/j.tws.2013.04.003.
93) A. Eyvazian, H. Mozafari, and A.M. Hamouda, "Experimental study of corrugated metal-composite tubes under axial loading," *Procedia Eng.*, **173** 1314–1321 (2017).
94) R. Subbaramaiah, B.G. Prusty, G.M.K. Pearce, S.H. Lim, and R.S. Thomson, "Crashworthy response of fibre metal laminate top hat structures," *Compos. Struct.*, **160** 773–781 (2017). doi:10.1016/j.compstruct.2016.10.112.
95) R. Subbaramaiah, G. Prusty, G. Pearce, S.H. Lim, D. Kelly, and R. Thomson, "A feasibility study for multi-material retrofittable energy absorbing structure for aged helicopter subfloor," *28th Congr. Int. Counc. Aeronaut. Sci. 2012, ICAS 2012*, **6** 4988–4995 (2012).
96) H.W. Song, Z.M. Wan, Z.M. Xie, and X.W. Du, "Axial impact behavior and energy absorption efficiency of composite wrapped metal tubes," *Int. J. Impact Eng.*, **24** (*4*) 385–401 (2000). doi:10.1016/S0734-743X(99)00165-7.
97) Z. Zhang, and F. Taheri, "Numerical studies on dynamic pulse buckling of frp composite laminated beams subject to an axial impact," *Compos. Struct.*, **56** (*3*) 269–277 (2002). doi:10.1016/S0263-8223(02)00012-0.
98) Z. Zhang, and F. Taheri, "Dynamic damage initiation of composite beams subjected to axial impact," *Compos. Sci. Technol.*, **64** 719–728 (2004). doi:10.1016/j.compscitech.2003.07.002.